THE DISTRIBUTION OF THE ORBITS OF SPORADIC METEORS

By A. A. Weiss*

[*Manuscript received September* 6, 1956]

Summary

The directions of the reflection points of sporadic meteor trails for March and September 1953, and the hourly echo rates of sporadic meteors obtained from the Adelaide radio survey of meteor activity over 1952–1956 are analysed. Diurnal and annual variations in the sporadic echo rate are predicted from contemporary theory on the reflection of radio waves from meteor trails for several model distributions. A sporadic distribution is derived which consists of a concentration of direct short-period orbits to the plane of the ecliptic superimposed upon a more uniform distribution of near-parabolic orbits. This distribution is consistent with the results of radar, visual, and telescopic surveys in the northern hemisphere. The density of sporadic meteors round the Earth's orbit is also derived.

I. Introduction

The diurnal and annual variation in the visual rate of detection of sporadic meteors has been known for many years, but until recently the interpretation of these variations has been a matter for controversy. This is so because the number of sporadic meteors detected visually is determined, apart from the luminosity function and subjective factors, jointly by the distribution of orbits in space and by the velocity distribution. The assumption of uniform distribution led to the postulated hyperbolic component of sporadic meteors. The development of the radio echo techniques for the detection of meteors, and especially the extensive radio measurements of geocentric velocities of sporadic meteors in England and Canada, which do not support the existence of the hyperbolic orbits, has led to a reappraisal of the problem of the distribution of sporadic meteors.

Investigations made prior to 1954 have been summarized by Lovell (1954, p. 96). Continuous radio surveys of echo rates made at Jodrell Bank during 1949–1951 indicate a strong concentration of sporadic orbits to the plane of the ecliptic, with a preponderance of direct orbits with high eccentricity. A similar concentration to the ecliptic is found by Prentice using visual techniques in which individual meteors are observed from two stations simultaneously. The ecliptical component moving in direct orbits also affords an explanation of Hoffmeister's visual counts without reference to a hypothetical hyperbolic component.

More recently, Kresák (1955) in Czechoslovakia has demonstrated that the concentration of sporadic meteor orbits to the plane of the ecliptic, and the

* Division of Radiophysics, C.S.I.R.O., at Department of Physics, University of Adelaide.

prevalence of direct over retrograde motions, extends to the fainter telescopic meteors. There is a possibility that the ratio of direct to retrograde motions is larger for telescopic than for visual meteors. Levin (1955) also finds a very large excess of direct over retrograde motions amongst both visual and telescopic meteors down to the 10th magnitude.

The apex and antapex velocity experiments of Almond, Davies, and Lovell (1953) show that, in addition to a concentration to the ecliptic, there is a random distribution of meteors with low heliocentric velocities (~35 km/sec). Preliminary reports on the three-station technique of Davies and Gill (Kaiser 1954 ; Bok 1955), which yields orbits of individual meteors, suggest that many of the fainter meteors (limiting magnitude 7 or 8) move in short-period orbits of low eccentricity, amongst which high inclinations to the ecliptic are common. Once again direct motions predominate.

Although this account is not exhaustive, enough evidence has been marshalled to show that the distribution of sporadic meteors probably consists of a concentration of predominantly direct orbits near the plane of the ecliptic superimposed upon a distribution more uniform in heliocentric coordinates.

Of the data on which these investigations were based, only Hoffmeister's visual observations were made in the southern hemisphere. During a radio survey of meteor activity at Adelaide, extensive data on sporadic meteor activity have been accumulated. The " wind " equipment used has been fully described by Robertson, Liddy, and Elford (1953), and some preliminary work on the interpretation of the sporadic counts has appeared (Weiss 1955).

The direction-finding system incorporated in the equipment gives the directions of reflection points of meteor trails. Since these directions are determined, within limits which are described, by the radiants of the meteors producing the detected trails, some direct information on the distribution of radiants of sporadic meteors is obtained. The hourly rate of detection of sporadic meteors is the other raw material collected. The evaluation of the sporadic rate is a necessary preliminary to the determination of shower activity, which is the primary object of the survey. But, in addition to this, radar counting is objective and does not suffer from the uncertainties involved in the subjective visual counting method, although the interpretation of the radar counts is still difficult. There is also the very great advantage of continuity in the radar counts.

The analysis of direction data, and the interpretation of radio counts of sporadic activity over the period 1952–1956, together give a consistent picture of the distribution of sporadic meteors detected over Adelaide. It is satisfactory that this distribution agrees with that suggested by the other researches reviewed above.

Since only major meteor showers can be recognized and subtracted from the total counts, the term " sporadic meteors " here embraces both minor meteor showers not resolved by the equipment and meteors pursuing isolated paths round the Sun.

II. The Distribution of Radiants of Sporadic Meteors

The direction data analysed in this section are the azimuths and zenith angles of reflection points of individual meteor trails, relative to the observing station. These are calculated from the direction cosines of the reflection points, measured by the direction-finding system of the equipment.

On the assumption of specular reflection, the possible reflection points corresponding to a given radiant will lie on the intersection with the celestial sphere of the plane passing through the station origin (mid point of transmitter-receiver base line) perpendicular to the line joining the station origin to the radiant point. These possible reflection points are further limited by the aerial polar diagram. For the present application this has maximum gain at the zenith, and falls off uniformly, and almost independent of azimuth, to a zero near zenith angle 50°. No reflection points should be expected at zenith angles greater than 50° and in fact very few (~1 per cent.) are found. A further restriction on the possible reflection points is imposed by the method of measurement of the direction cosines. This requires several cycles of Doppler beat between sky and ground waves. As it has been established that the winds which shift the phase of the sky wave have no significant vertical component, reflections at low zenith angles can produce only very low Doppler frequencies, and the echo decays before the requisite number of Doppler cycles have been recorded. Hence very few reflection points are found at low zenith angles, as is evident from Figure 4.

Because of these restrictions on zenith angles, reflection points corresponding to a given radiant should fall within a fairly narrow band of azimuths, whose centre is shifted 180° from the azimuth of the radiant. This expectation is confirmed by measurements on the Geminid radiant (diameter <4°) in 1952 and 1953.

The azimuths of the reflection points of 580 echoes detected over the peak of the Geminid activity, from 23 to 05 hr, have been determined. About a third of these echoes are due to sporadic meteors, but the peaks in the azimuth distributions, due to true Geminid meteors, are very clearly defined. The centres of the azimuth bands for the Geminid echoes, measured in hourly groups, are plotted in Figure 1, along with the relation between observed azimuth and time found from them by the method of least squares. The expected mean azimuth for a radiant of declination +32° is also shown. Considering the small number of echoes involved, and the disturbing effect of the sporadic background, it is evident that the reflection points are in fact diametrically opposed to the azimuth of the radiant.

This fact can now be applied with confidence to the determination of directions of arrival of sporadic meteors from the measured reflection points.

As indicated above, the distribution of zenith angles of reflection points is determined largely by the aerial polar diagram and the method of measurement, and the zenith angle of the radiant is of minor importance. Analysis of the Geminid echoes shows that the mean zenith angle of reflection points increases, but only slightly, as the elevation of the radiant increases from 0 to 23°.

The azimuths of the reflection points for some 1600 echoes detected during March and September 1953 have been divided into 30° sectors at 2-hourly intervals. The resulting distributions are drawn in Figure 2. These samples are entirely free of shower echoes. An examination of the possible effects of the wind pattern on the observed distributions has been made, with negative result. These distributions thus depict an inherent property of sporadic meteors.

The most striking feature of the distributions for the two months is their similarity. The dominant feature in both months is the rotation, through 360° in 24 hr, of the azimuth from which the smallest number of reflection points is detected. The rotation is in the same sense as, and in phase with, the rotation

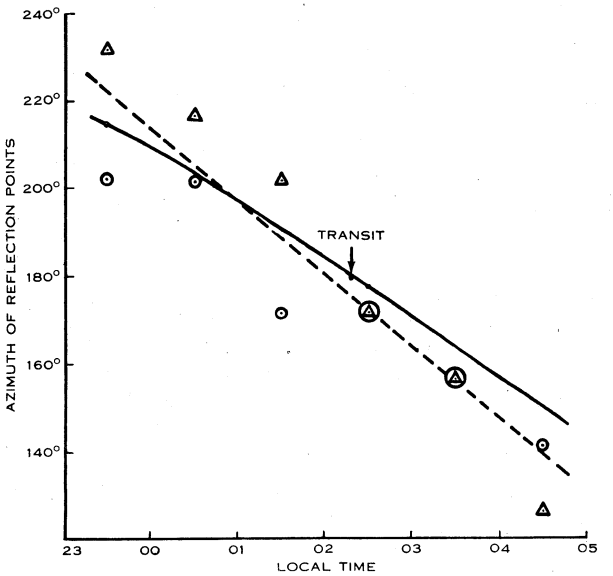

Fig. 1.—Azimuths of reflection points of Geminid echoes. Observed azimuths – – –; △ 1952; ⊙ 1953. Expected azimuths for radiant at Dec. +32° ——.

of the azimuth of the apex of the Earth's way. This is more clearly brought out in Figure 3, in which the positions of the observed minima are compared with the azimuth of the apex for each month separately.

Since it is obvious, from what has been said above, that no reflection points can be detected in the direction of a radiant, the radiants of sporadic meteors are evidently concentrated towards the direction of the apex. The fact that the correspondences of Figure 3 persist whilst the apex is below the horizon suggests that the concentration is comparatively broad.

The occurrence of peaks in the distributions at azimuths near east and west, close to sunrise and sunset, further suggests the presence of helion and anti-helion concentrations amongst the apparent sporadic radiants. In fact these two components, along with the concentration to the apex, give a very good account of the detail of Figure 2. From the zenith angle distributions of Figure 4, it is apparent that the azimuth distributions will be dominated by those sources

which are low in the sky at the time. For example, the sequences 04–06–08 hr and 16–18–20 hr are dominated by the helion and antihelion components which give reflection points to east and west. The rapid swing from easterly reflection

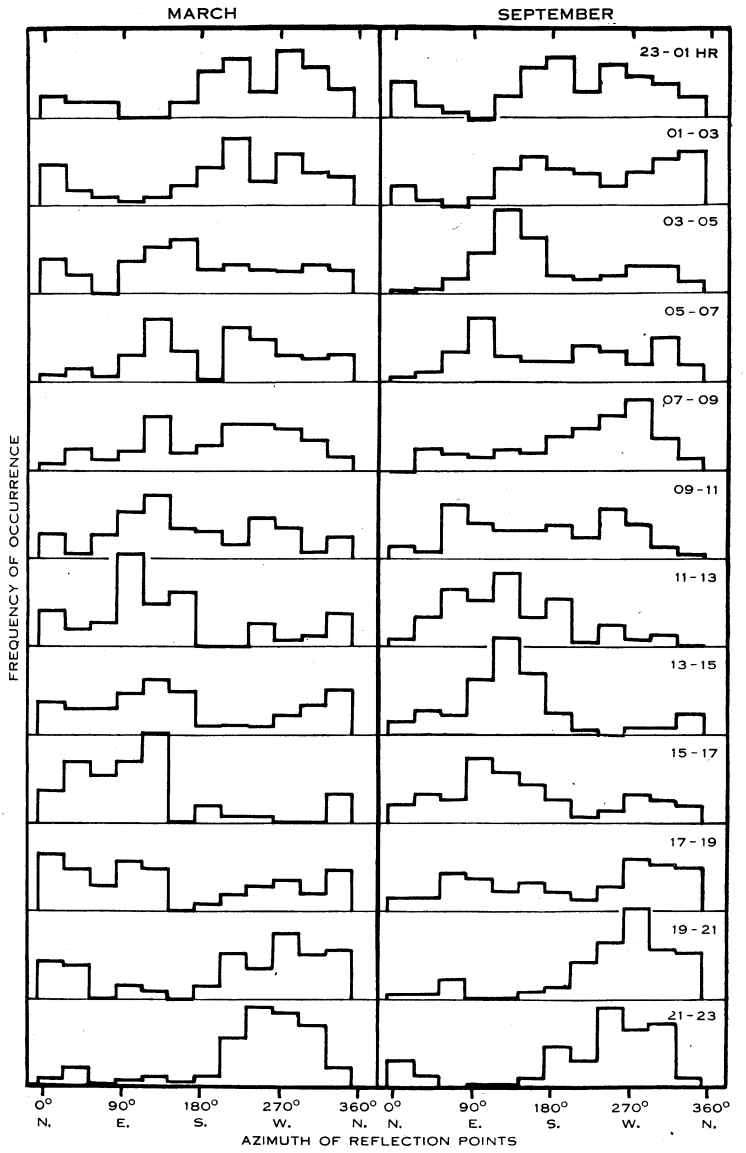

Fig. 2.—Distribution of azimuths of reflection points of sporadic echoes, March and September 1953.

points at 04 hr to westerly reflection points at 08 hr is due to the setting of the antihelion component and the rising of the helion component. A similar swing from east to west over 16–20 hr is due to the setting of the helion component and the rising of the antihelion component. Westerly reflection points near

midnight, and easterly near midday, are associated with the rising and setting of the apex component.

The rapidity of the east-west swings near sunrise and sunset suggests that the helion and antihelion concentrations are relatively sharp, much more so than the concentration to the apex.

As is to be expected, very little is added to these conclusions by the analysis of the zenith angles of the reflection points. The distributions are given in Figure 4. The mean zenith angle per 2-hr interval varies by less than 7°

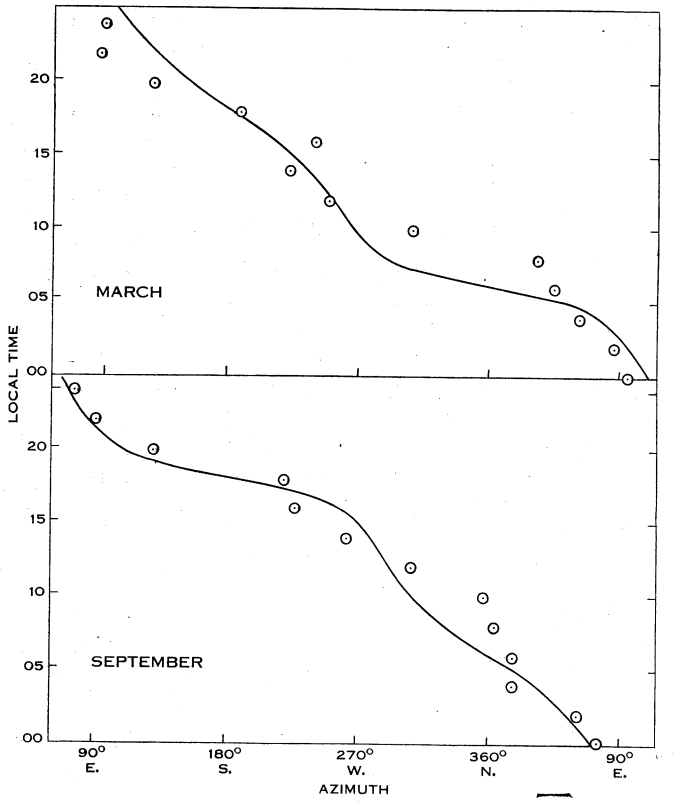

Fig. 3.—Comparison between azimuth from which the number of reflection points is a minimum ⊙ ; and the azimuth of the apex of the Earth's way ——. Sporadic meteors, March and September 1953.

throughout the day, and once again the variation is very similar as between March and September. The movement of the mean zenith angle throughout the day is substantiated by the variation in the ratio (number of zenith angles $\leqslant 20°$/number of zenith angles $\geqslant 40°$), and there is no doubt that there are more reflection points with low zenith angles near sunrise and sunset than at other times throughout the day. This is probably connected with the presence near the horizon of the sharp intense helion and antihelion concentrations, at these times.

The zenith attraction on the radiant of a meteor moving with parabolic velocity and detected near the horizon, at elongation 90° from the apex, is less

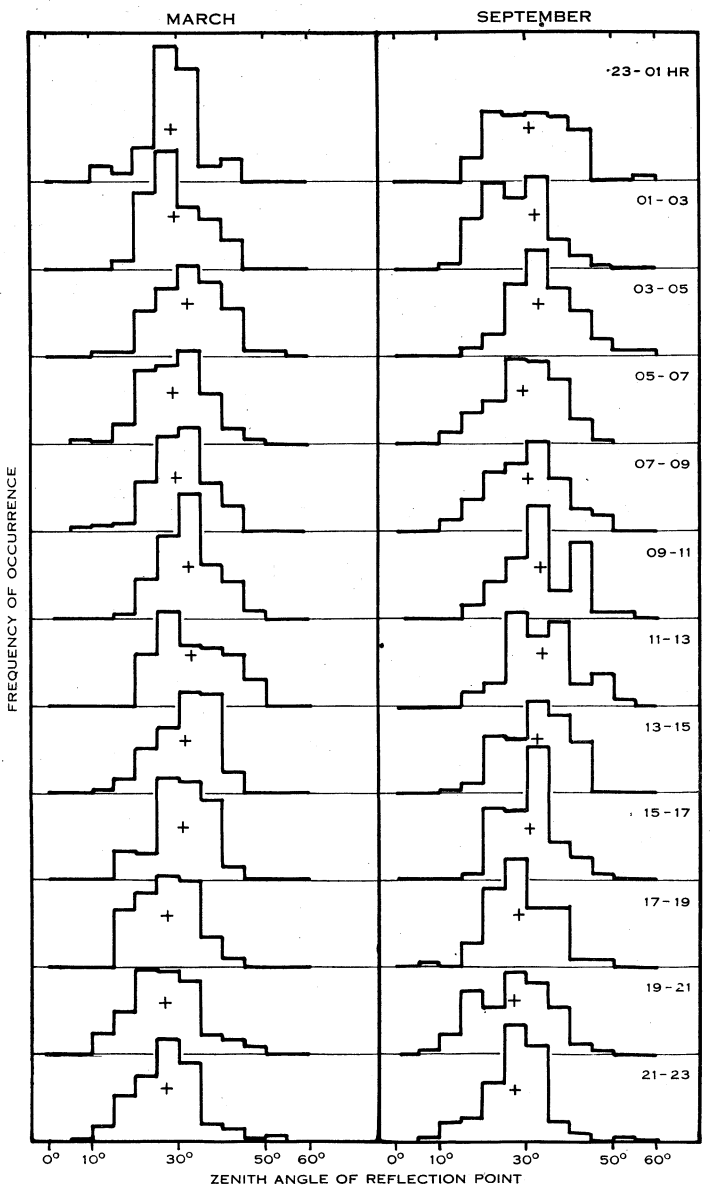

Fig. 4.—Distribution of zenith angles of reflection points of sporadic echoes, March and September 1953. + Mean zenith angle per 2-hr interval.

than 4°. For a short-period orbit, with a heliocentric velocity of 35 km/sec, the zenith attraction is larger, near 10°. In view of the magnitude of these corrections, the apparent symmetry of the helion and antihelion concentrations

about the times of sunrise and sunset is understandable. The zenith attraction near the apex is at all times negligible.

The limiting electron density for echoes detected at zenith angle 30° is 3×10^{11} (Fig. 7). This corresponds to radio magnitude $M_r=6\cdot3$, according to the definition of Browne *et al.* (1956). The distribution of sporadic radiants outlined above therefore relates to meteors brighter than the sixth magnitude.

The directions of the reflection points of sporadic meteors measured during the equinoctial months of March and September have demonstrated the existence of concentrations of radiants towards the directions of the apex, the Sun, and the antisun. Dominance of the records for the solstitial months of June and December by showers has precluded a similar analysis for these months. However, in view of the numerous reports of the apex and antihelion components by visual and telescopic workers, there is no reason to doubt that the source distribution found here for March and September will hold throughout the year.

The significance of this radiant distribution is taken up in Section VI.

III. The Observed Sporadic Echo Rate

The equipment has been in effective operation for counting meteors since June 1952. It has been operated semi-continuously since then, the shortest run being 3 weeks and the longest 8 months. Every month of the year has been surveyed at least once, some three times.

The basic material is the number of echoes detected each hour, as counted from the films. As far as possible, echoes from shower meteors have been excluded, but the identification of showers near the limit of resolution is uncertain. The equipment has not been maintained at the ideal of constant sensitivity over the whole period June 1952 to April 1956, but every effort has been made to hold the sensitivity constant for months at a time. The data can be divided into five groups, within each of which the sensitivity has remained unaltered, although as between groups it has varied by factors of 1·8 or less.

The hourly echo rates have been analysed by months to establish the mean diurnal variation for each month separately. The diurnal curves are drawn in Figure 5 ; these are the actual counts not corrected for equipment sensitivity at the time. Attention is drawn to the asymmetry of many of these curves, to the tendency for flat minima and sharper maxima, and to the occurrence of many subsidiary maxima. Another striking feature is the general similarity of the diurnal variation for a given month from year to year, and the repetition of much of the finer details of the variation, e.g. the months of May, November, and December.

The sporadic meteors included in this rating survey are those brighter than radio magnitude $M_r=7\cdot5$.

The annual variation of the ratio of maximum to minimum hourly echo rate in the diurnal variation is plotted in Figure 6 (*a*). Also shown, in Figure 6 (*b*), is the average echo rate per day for each month ; the annual variation in

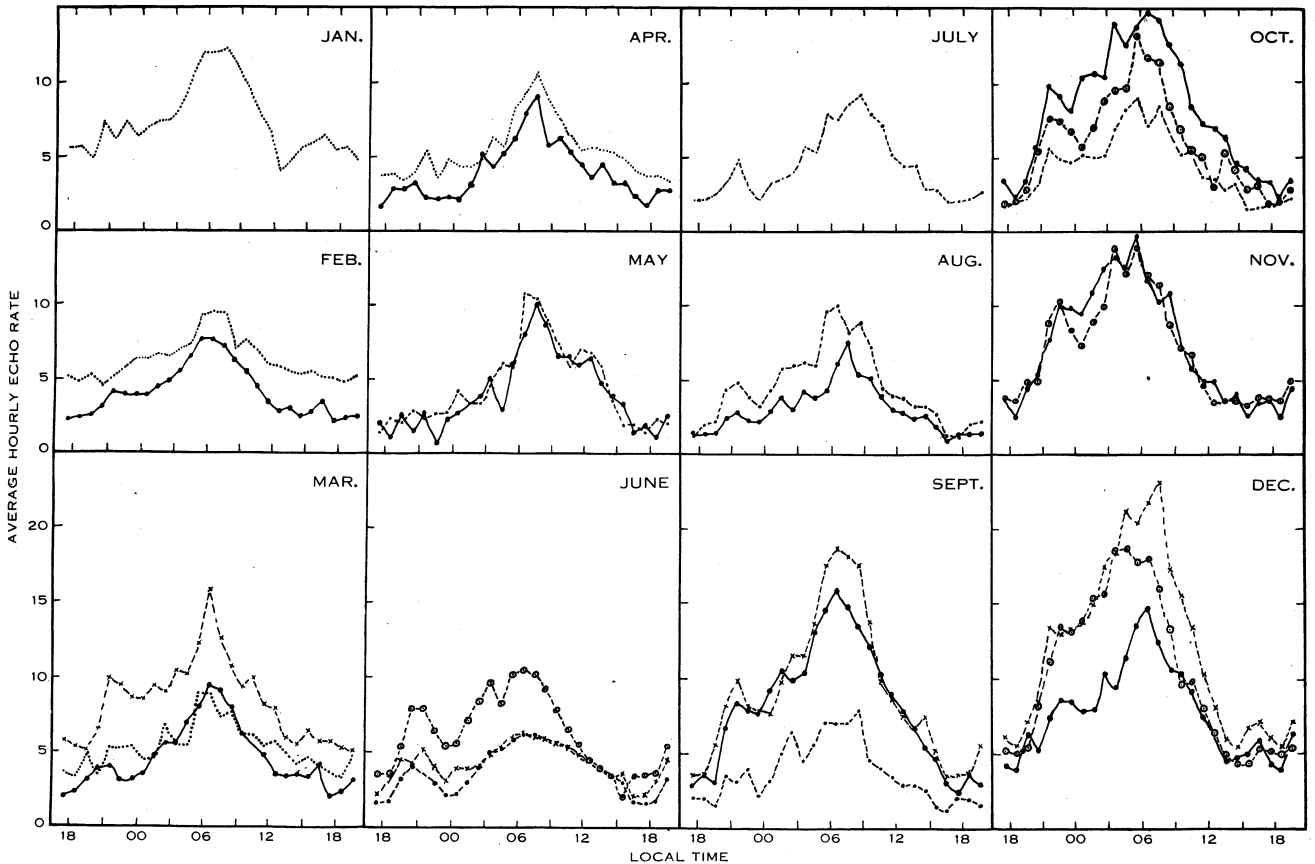

Fig. 5.—Diurnal variations in observed sporadic echo rates. Echo rates have not been corrected for equipment sensitivity.
1952 ○ – – – ○; 1953 ×– – –×; 1954 ● – – – – ●; 1955 ——; 1956 · · · · ·.

this quantity is small. These average echo rates per day have been corrected for equipment sensitivity by combining information from different runs (at different sensitivities) by a method of successive approximations. The validity of this procedure is examined in Section IV (*d*).

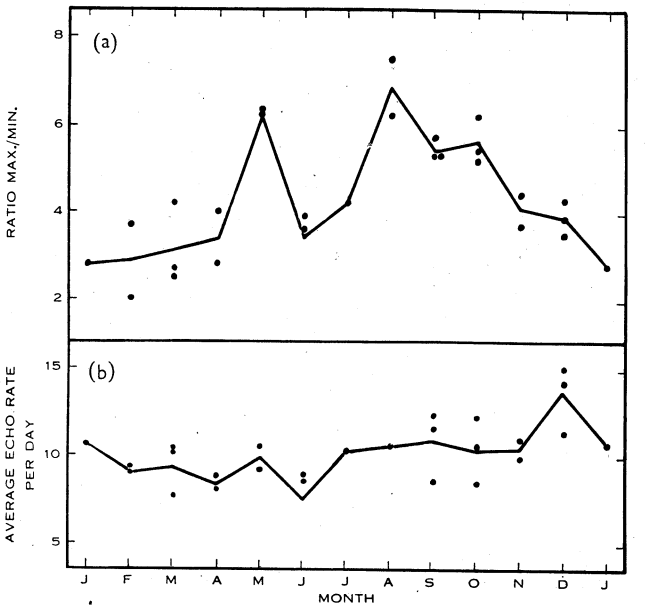

Fig. 6.—Annual variations in observed sporadic echo rates. (*a*) Ratio of maximum to minimum hourly echo rate in the diurnal variation. (*b*) Average echo rate per day, corrected for equipment sensitivity.

IV. Echo Rate as a Function of Zenith Angle of Radiant

The actual counts of sporadic meteors, when freed from the variations imposed by the characteristics of the detecting equipment, may be used to supplement the information on the spatial distribution of sporadic meteors which is contained in the radiant distributions derived in Section II. We clearly have to deal with a source of sporadic meteors anisotropically distributed over the whole of the celestial sphere. For the purposes of analysis such a distributed source may be divided into a large number of small radiant areas, whose dimensions are of the same order as the small radiant areas of shower meteors.

The first step in the interpretation of the sporadic counts is to reach an understanding of the way in which the rate of detection of shower meteors depends upon the zenith angle and azimuth of the radiant. A good deal of information on this dependence has been accumulated from showers observed at Adelaide, but in addition to this it has been felt worth while to attempt to predict this dependence, from known equipment parameters and the physical behaviour of meteors in the Earth's atmosphere. The physical principles underlying the production and detection of meteor trails are now sufficiently

well established for a comparison between calculated and observed rates to be of considerable value, not only for its own sake but also because attention is thereby drawn to some of the inadequacies of contemporary theory.

It is appropriate to remark that the programme attempted in this section is complicated considerably by the existence of a minor lobe in the field of view of the equipment. Such minor lobes are undesirable for counting purposes, but were incorporated into the aerial pattern as part of the direction-finding system.

(a) Predicted Echo Rate from a Radiant

For Lovell-Clegg scattering, the line density of electrons/cm α_0 corresponding to a meteor detected at limiting sensitivity is

$$\alpha_0=\left(\frac{32\pi^2R^3\varepsilon}{PG_TG_R\lambda^3}\right)^{\frac{1}{2}}\left(\frac{mc^2}{e^2}\right), \quad \ldots\ldots\ldots\ldots\ldots \quad (1)$$

whilst for persistent echoes

$$\alpha_0=\left(\frac{54\pi^3R^3\varepsilon}{PG_TG_R\lambda^3}\right)^{2}\left(\frac{mc^2}{e^2}\right). \quad \ldots\ldots\ldots\ldots\ldots \quad (2)$$

In these expressions, and for the equipment in question,

P=transmitter power=250 W,
ε=minimum detectable echo power=3×10^{-14} W,
R=slant range to reflection point,
λ=wavelength=11·2 m,
G_T=transmitting aerial gain=9·5 max.,
G_R=receiving aerial gain=6·5 max.

With these equipment parameters, formulae (1) and (2) reduce to

$\alpha_0=10^9(R^3/G_TG_R)^{\frac{1}{2}}$ Lovell-Clegg scattering,
$\alpha_0=0\cdot62(R^3/G_TG_R)^2$ persistent scattering.

R is in kilometres, and the product G_TG_R max. has been normalized to 100. These expressions become equal when $\alpha_0=1\cdot2\times10^{12}$ electrons/cm, and are assumed to hold exactly for lower and higher electron densities respectively, although physically the change from one type of scattering to the other is neither rapid nor well marked.

Making use of theoretical aerial polar diagrams for the aerial systems as described by Robertson, Liddy, and Elford (1953), and of the concept due to Clegg (1948) of a meteor collecting zone at a definite height (here 90 km) which fixes R, the contours of α_0 shown in Figure 7 are obtained. On any contour, any meteor trail whose line density exceeds the α_0 appropriate to the chosen contour will be detected. It should be remarked at this juncture that the substitution of a thin collecting zone for the broader height distributions actually found for sporadic meteors (see e.g. Elford and Robertson 1953) will have little effect on contours for which $\alpha_0\leqslant10^{12}$, but may be serious for contours appropriate to

larger values of α_0, for which R is raised to the sixth power. The implication is that within the major lobe of the aerial pattern the assumption of a thin collecting zone is justified.

No allowance has been made for the enhancement of the reflection coefficient in transverse, as opposed to longitudinal, polarization of the incident wave. This effect can scarcely be important for distributed sources of radiants and need not be considered further at this stage.

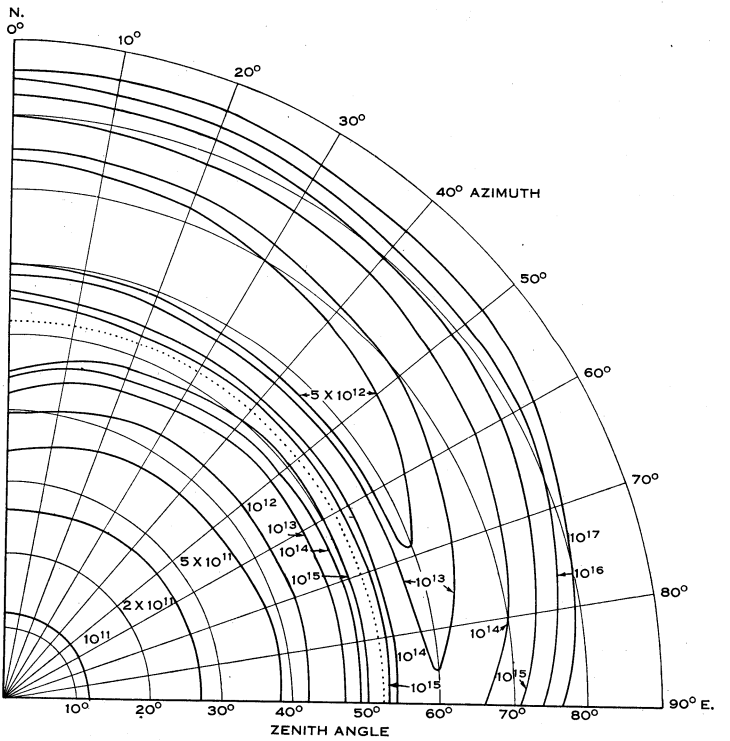

Fig. 7.—Theoretical sensitivity contours for the aerial system in use. The numbers marked against the contours are the values of the limiting electron densities α_0. A meteor echo is detected on (or within) a given contour if $\alpha > \alpha_0$.

Within the major lobe the contours are almost independent of azimuth, although a small asymmetry due to the non-coincidence of transmitting and receiving aerials has been ignored. The minor lobe is markedly asymmetrical.

The calculation of the echo rate expected from a radiant at a given zenith angle proceeds by determining the collecting area appropriate to the position of the radiant and integrating over this collecting area all incident meteors whose line densities exceed the limiting line densities defined by the contours of Figure 7. For a point radiant and a meteor collecting surface at a fixed height of 90 km above the Earth's surface, the collecting area degenerates into a line, the line forming the intersection of the 90-km spherical collecting surface and the plane perpendicular to the direction of the radiant from the observing station. This

geometry is imposed by the property of specular reflection of meteor trails (Section II).

The relation between the physical properties of the meteor and of the atmosphere, and the maximum line density α_{max}, may be written

$$\alpha_{max}=\frac{4}{9}\beta(\mu H)^{-1}m\cos\chi. \quad \ldots\ldots\ldots\ldots\ldots \quad (3)$$

The notation is that of Kaiser (1953): χ is the zenith angle of the radiant. For the moment the probability β of ionization of a single meteor atom is regarded as an invariant; this parameter is further examined in Section IV (*e*). Since μ and H are also essentially constant, (3) may be written

$$m_0=\text{const.}\ \alpha_0\beta^{-1}\sec\chi, \quad \ldots\ldots\ldots\ldots\ldots \quad (4)$$

and any meteor particle whose mass exceeds m_0 will be detected on (or inside) the contour α_0.

Following Kaiser (1953) we assume a mass distribution

$$\nu_m dm=\text{const.}\ m^{-s}dm, \quad \ldots\ldots\ldots\ldots\ldots \quad (5)$$

where ν_m is the flux of meteors with masses between m and $m+dm$. The echo rate is now calculated by integrating (5) over all masses above the limiting mass m_0 given by (4) and along the collecting line, denoted by L, defined earlier. Since the two integrations are independent, the echo rate as a function of zenith angle is given by

$$Z(\chi)=\text{const.}\ (\beta\cos\chi)^{s-1}\int_L \alpha_0^{1-s}dL. \quad \ldots\ldots\ldots \quad (6)$$

It has been assumed that s is a constant, independent of m. For sporadics, Browne *et al.* (1956) find $s=2$ for meteor radio magnitudes between 2 and 10. For showers there is evidence that s is slightly dependent upon radio magnitude, and may take values between about 1·5 and 2·5 for different showers.

The integration (6) has been performed within the limits of the major lobe of the aerial pattern (east-west section). It is sufficient to consider a flat collecting surface for meteors; the error in replacing the true spherical surface by a horizontal surface is less than 1 per cent. within the major lobe (elevation $>40°$), but is of course not justified at low elevations where the minor lobe is effective. The function Z is plotted in Figure 8 (*a*) for three values of s, namely, $s=1\cdot5$, $2\cdot0$, $2\cdot5$; the three curves have been normalized to $Z=1\cdot0$ at $\chi=70°$.

(*b*) *Observed Echo Rate from a Radiant*

By subtracting the estimated sporadic activity from the total counts during times of shower activity, the shower echo rate may be determined as a function of time and hence of zenith angle when the radiant coordinates are known. Data for five representative showers are given in Figure 8 (*b*). For radiant elevations up to 20°, the measured function Z is the same for all showers, and agrees quite well with the Z calculated for $s=2\cdot0$. For radiant elevations

exceeding 20° the measured functions Z for different showers diverge and do not fall off in accordance with predictions based on collection in the major lobe alone.

Before considering the effects of the minor lobe, it might be pointed out that the measured Z, especially for the Geminids, should correspond to an s-value somewhat less than 2. Part of the discrepancy may be due to neglect of

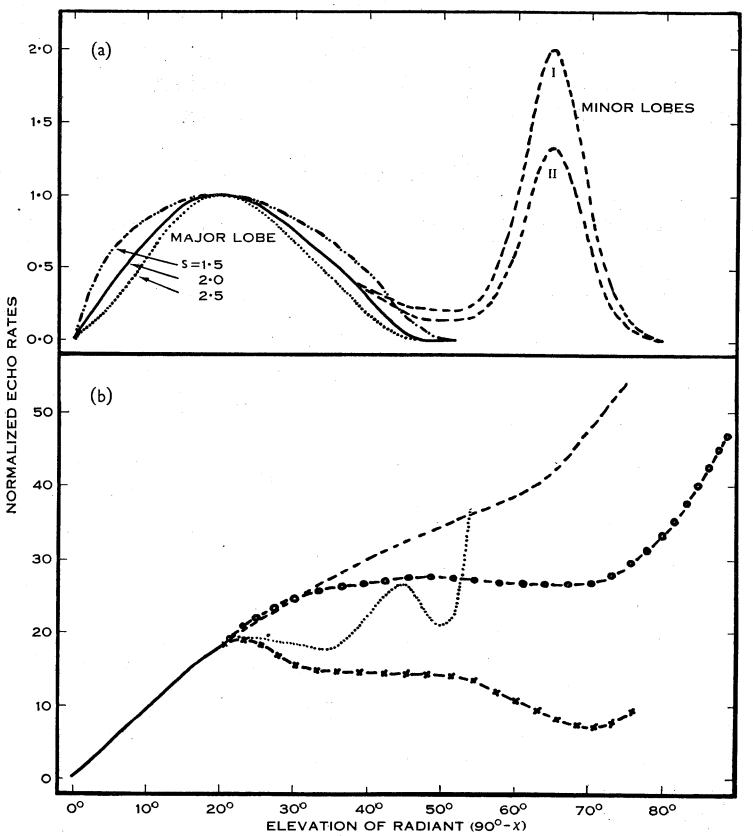

Fig. 8 (*a*).—Predicted echo rate from a point radiant as a function of the elevation of the radiant, for several aerial polar diagrams.

Fig. 8 (*b*).—Echo rates observed for showers. Corona Australids 1953 (Dec. —50°) – – –; η-Aquarids 1954 (+01°) · · ·; December shower 1955 (—36°) o–o–o; δ-Aquarids 1954 (—21°) ×–×–×; Geminids 1952 and 1953 (+32°) ——.

the minor lobe, but a more likely explanation is the failure of the assumption, implicit in the derivation of (**6**), that every meteor for which $\alpha > \alpha_0$ is detected by the equipment. The validity of this assumption is examined in Appendix I, where it is concluded that some detectable echoes are missed at small elevations of the radiant. Allowance for this will reduce the discrepancy between measured and calculated Z.

(*c*) *Effects of the Minor Lobe*

A rough calculation based on the contours of Figure 7 suggests that for a radiant culminating at a zenith angle of 6° the expected echo count, on the scale of Figure 8 (*b*), is about 40. For zenith angle 15°, the expected count is about 50. These are within the limits actually observed.

The predicted minor lobe is narrow, centred on zenith angle 65°. Analysis of the measured Z suggests that the minor lobe actually is as narrow as predicted, but is displaced in elevation by site errors which are in the sense expected from the aerial surroundings. For this reason, accurate calculations of the contribution of the minor lobe to the theoretical function Z have not been made, although the problem has been solved and applied in another connexion.

The different contributions from the minor lobe to the functions Z measured for the showers shown in Figure 8 (*b*) is partly an effect of the different zenith angles at culmination. However, the major part of the differences, including the lack of any maximum near 20°, is due to the movement of the radiant in azimuth as well as in zenith angle. It is clear from Figure 7 that for low and moderate radiant elevations the contribution of the minor lobe is larger for azimuths near east-west than those near north-south.

For certain radiant positions the contribution of the minor lobe to the echo rate is as great as, or exceeds, that of the major lobe. Having regard to the fact that sporadic meteors form a distributed source in which many zenith angles and azimuths are represented simultaneously, two functions Z, both independent of azimuth, have been used for computations on the minor lobe in later sections. These are the curves labelled I and II in Figure 8 (*a*). They are in the theoretical position (zenith angle 65°) and their amplitudes are approximately those needed to explain the diurnal variations in the actual sporadic meteor counts. Because of smoothing by the distributed source and the broad aerial beam, the exact shape of Z for the minor lobe is unimportant.

Although not relevant to the main topic, it might be pointed out here that the activity of a shower at transit may be strongly influenced by detection in the minor lobe. Comparative shower rating is only possible by confining attention to the rates when the radiant elevation is less than 20°.

(*d*) *Effects of Equipment Sensitivity*

Kaiser (1953) has defined an equipment sensitivity factor

$$F=(P\lambda^3/\varepsilon)^{\frac{1}{3}}.$$

For a constant aerial polar diagram, the number of echoes N detected is a function of F, thus :

$$\left.\begin{array}{ll} N \propto F^{s-1} & \text{Lovell-Clegg scattering,} \\ N \propto F^{4(s-1)} & \text{persistent scattering.} \end{array}\right\} \quad \ldots\ldots\ldots \quad (7)$$

These expressions follow directly from (**6**), (**1**), and (**2**); a small correction introduced by the finite meteor height distribution has been ignored.

Attention has been drawn by Bullough (1954) to the necessity for considering the different values of s appropriate to shower and sporadic meteors when

reducing echo rates to a common epoch. Since we are here only concerned with sporadic meteors, $s=2$ and the expressions (7) become $N \propto F$ and $N \propto F^4$ respectively. The great majority of echoes detected within the major lobe are of the Lovell-Clegg type, but within the minor lobe only persistent echoes are detected. This implies that the minor lobe is much more sensitive to small changes in equipment sensitivity than the major lobe. The Corona Australid shower in particular affords verification of this.

The fact that showers exhibit greater sensitivity to changes in F than sporadic meteors indicates that collection of the latter occurs mainly in the major lobe. Moreover, the repetition of the characteristic features of the diurnal variations shown in Figure 5 from year to year at different equipment sensitivities suggests little relation between collecting area and sensitivity.

After eliminating the annual variation from the sporadic counts of Section III, the echo rate has varied by a factor of less than 2 over the period of the survey. This variation is sufficiently small that these data may be reduced to a common equipment sensitivity by taking simple proportionality between N and F. This procedure is of course justifiable only over the narrow range of equipment sensitivity actually used.

(e) *Effects of Meteor Velocity*

The relation between the ionizing efficiency β and the velocity v of the meteor particle may be described by the power law $\beta = \text{const.}\ v^n$. The value of the exponent n is not known at all well. Evans and Hall (1955) by an indirect method involving height distributions find $n = 0 \cdot 5 \pm 0 \cdot 5$ for sporadic meteors. At the other extreme, Whipple (1955) finds $n \sim 5$ from the relative frequencies of occurrence of radio and bright photographic meteors (sporadics).

The value of n is of little consequence in the case of shower meteors unless absolute fluxes are in question. Since the velocities of shower meteors are sharply concentrated to a mean value, β may be replaced by a constant which will differ from shower to shower, and the only result is an alteration in the scale factor of Figure 8. In the case of sporadic meteors, however, a broad velocity distribution depending upon elongation of the radiants from the apex may be expected. Hence β must be replaced by a weighted sum which may depend upon position as well as upon time. Since $s=2$, v enters to the power n (see expression (6)). Should n prove to be large, any marked diurnal changes in the distribution of sporadic geocentric velocities must be reflected in the diurnal variation in counts of sporadic meteors. At the present time little can be done beyond drawing attention to this possibility, and noting that a lower limit is set to the ratio of direct to retrograde orbits by the assumption that β is, in fact, independent of v.

V. The Predicted Sporadic Echo Rate

Knowing the echo rate expected from a point source at any position on the celestial sphere, the calculation of the echo rate expected from any distribution of sporadic radiants over the celestial sphere is quite straightforward. The distribution of sporadic radiants over the celestial sphere depends upon the

distribution of sporadic orbits in space, upon their velocity distribution, and upon the Earth's motion. In predicting rates it is not necessary to assume a distribution in space at the outset; it may be more convenient to postulate an apparent distribution of radiants over the celestial sphere. However, the interpretation of such apparent distributions requires a knowledge of the velocity distribution.

It would of course be preferable to use the observed sporadic counts of Section III, in conjunction with the function Z of Figure 8, to derive the apparent distribution of sporadic radiants over the celestial sphere. Unfortunately, the aerial pattern is not sufficiently well known to meet the stringent requirements of this analytical approach. The best that can be done is to assume various models for the sporadic distribution and compare them with the actual counts. Even if the analytical approach were possible, aerial smoothing by the broad aerial beam would suppress much of the finer detail of the distribution. For the same reason, there is a limit to the fine structure which need be incorporated in the model distribution.

Two types of model distribution are considered. The first is a line distribution of apparent sporadic radiants round the ecliptic, which is an idealization of a sharp concentration towards the ecliptic. The second is a more uniform distribution over the whole of the celestial sphere.

(*a*) *Ecliptical Concentration* (*Model E*)

We define an apparent source strength σ, distributed as a line source round the ecliptic, which has the value $\sigma=4$ over the 180° of ecliptical longitude centred on the apex, and the value $\sigma=1$ along the remainder of the ecliptic. This distribution is tied to the apex and, relative to an observer on the Earth, it rotates completely round the ecliptic once in 24 hr. The sporadic echo rate at any time is found by forming $\oint \sigma Z \mathrm{d}E$, where $\mathrm{d}E$ is an element of the ecliptic and the integral is taken right round the ecliptic. The diurnal and annual variations are built up by allowing the source and the ecliptic to perform their daily and annual movements.

Calculations with model E have been made using three forms of the function Z, namely, major lobe alone with $s=2$, and major lobe plus minor lobes I and II (Fig. 8 (*a*)). Diurnal variations throughout the year for the case of major+minor lobe II are given in Figure 9. The form of these curves is much the same for all of the aerial patterns considered; the asymmetries are an effect of the motion of the ecliptic, not of the inclusion of the minor lobe. The ratio of maximum to minimum hourly echo rate in the daily variation and the annual variation in the average daily echo rate are shown in Figure 10. The scale of Figure 10 (*a*) is arbitrary; this diagram illustrates the contribution made to the total rate by the minor lobe.

(*b*) *Uniform Distributions* (*Models U*)

These models are based on the hypothesis of a uniform distribution of sporadic meteors in space. The apparent distribution over the celestial sphere is found by applying corrections for the motion of the Earth (towards the

direction of the apex) and for the number of meteors intercepted by the Earth. These corrections, which depend upon the apparent elongation of the radiant from the apex and upon the heliocentric velocity of the meteor, are given by Lovell (loc. cit., p. 117). The direction of the apex from the observing station

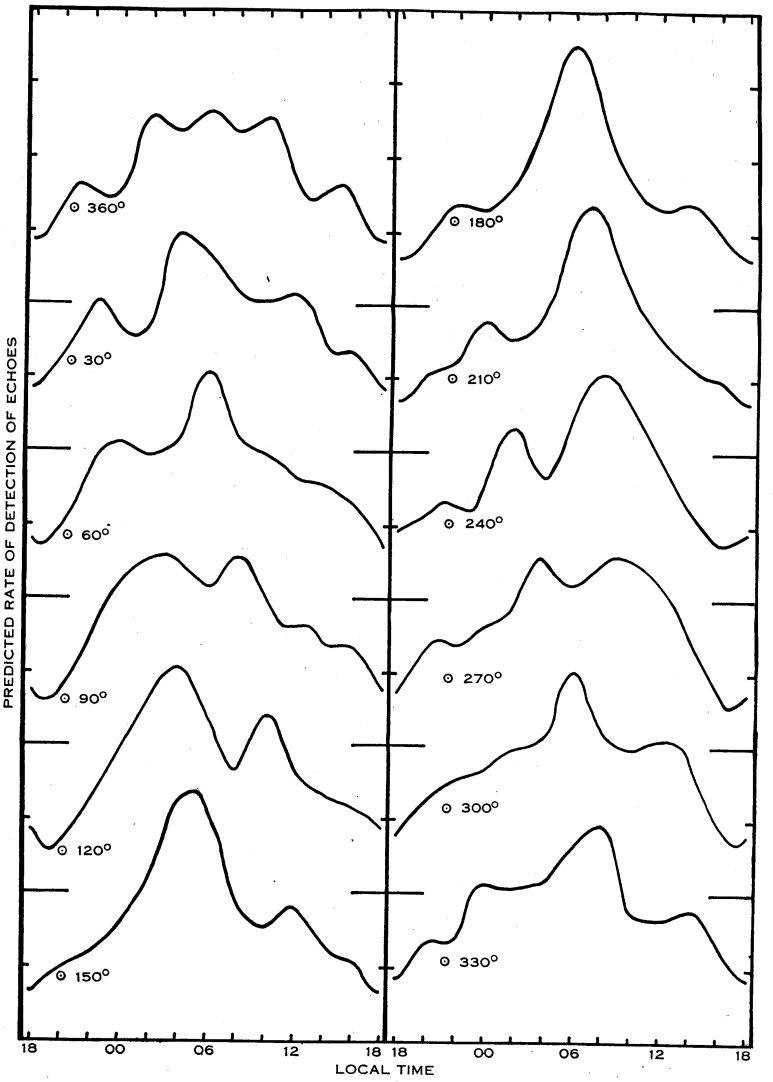

Fig. 9.—Diurnal variations in echo rate predicted for an ecliptical source distribution of sporadic meteors (model E). Aerial pattern: major lobe + minor lobe II.

constitutes an axis of symmetry for the problem, and the expected rate of sporadic meteors collected from the whole of the visible hemisphere is obtained as a function of the zenith angle of the apex. The relation between zenith angle of the apex and hour angle of the Sun (Davidson 1914) is then used to obtain the

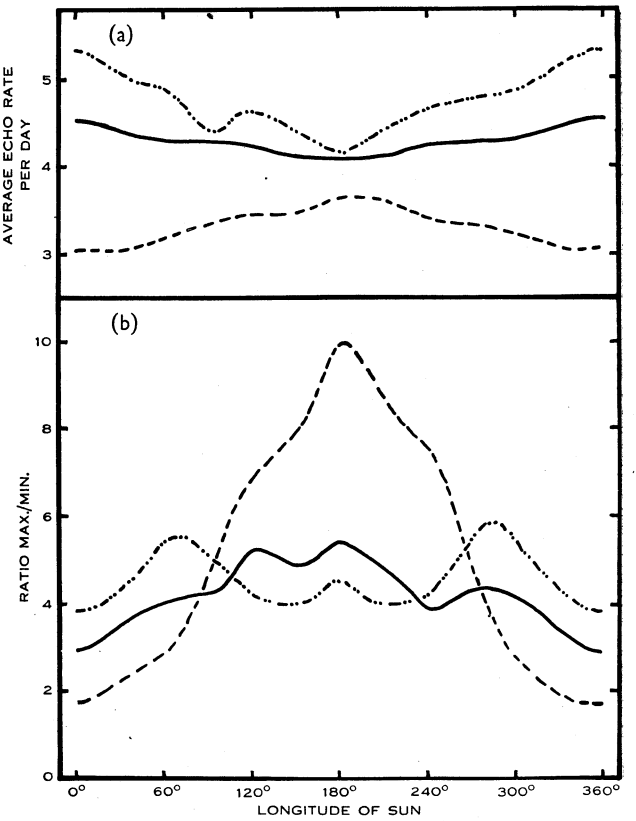

Fig. 10.—Annual variations in echo rate predicted for model E. Major lobe only – – –; major lobe+minor lobe I –·–·–·–; major lobe+minor lobe II ——.

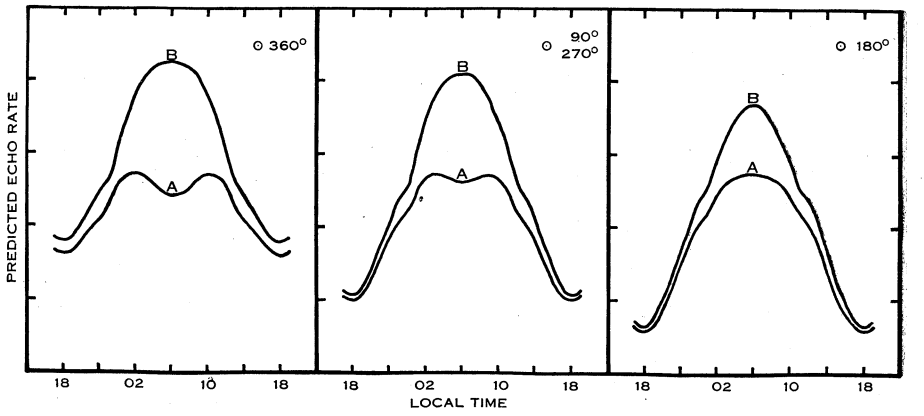

Fig. 11.—Typical diurnal variations in echo rate predicted for a uniform space source distribution of sporadic meteors with parabolic velocities (model U_{42}). Curves *A*, major lobe only; curves *B*, major lobe+minor lobe II.

diurnal and annual variations in the predicted rate. Zenith attraction has not been taken into account.

Computations have been carried through for two heliocentric velocities, 42 and 35 km/sec. These models are denoted by U_{42} and U_{35} respectively.

Typical diurnal variations are shown in Figure 11, with and without the contributions from minor lobe II. Without exception, model U curves are symmetrical about 06 and 18 hr. Figure 12 depicts the ratio of maximum to minimum hourly echo rate in the diurnal variation throughout the year. The annual variation in the average echo rate per day has not been illustrated. It is almost independent of the model and of the aerial pattern, the activity being highest during March ($\odot$=360°), when it exceeds the September activity by 30 to 40 per cent.

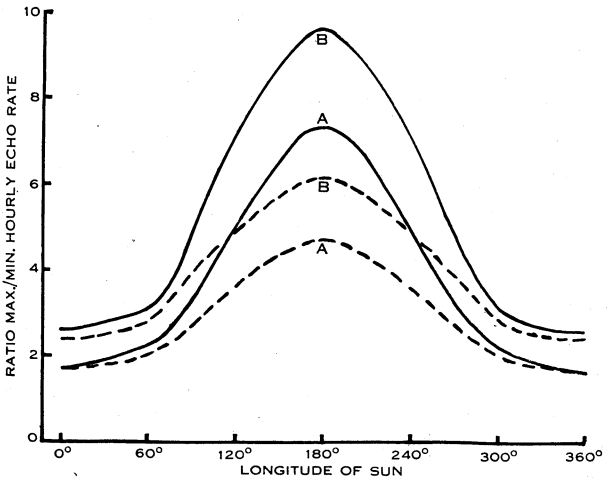

Fig. 12.—Annual variation in the ratio of maximum to minimum hourly echo rate in the diurnal variation predicted for uniform space models. Model U_{35} ——; model U_{42} – – –. Curves *A*, major lobe only; curves *B*, major lobe+minor lobe II.

VI. Interpretation of the Observations

The measurements of reflection points described in Section II constitute direct evidence for a helion component of sporadic meteors. The existence of such a component had already been inferred, indirectly, from counts of sporadics at Jodrell Bank. The antihelion component was known from visual, telescopic, and radar observations.

The helion, antihelion, and apex concentrations together point to a component in the sporadic distribution which is concentrated to the plane of the ecliptic. However, from the manner in which the azimuth of the minimum number of reflection points follows the azimuth of the apex it is clear that there must be an additional component more uniformly distributed over the celestial sphere. For otherwise very few reflection points would lie in directions close to north, a situation not supported by Figure 2. If it is accepted that portion of the concentration to the apex is the effect of the Earth's motion distorting a

uniform distribution of sporadic meteors, then the apparent distribution found for the ecliptical component—marked helion and antihelion concentrations with fewer apparent radiants in the directions of the apex and antapex—implies a predominance of direct orbits of short period amongst those orbits confined to the plane of the ecliptic.

The direction data thus point to a distribution of sporadic meteors observed in the southern hemisphere which agrees with that found for the northern hemisphere. This distribution may therefore be used with confidence in the interpretation of the sporadic counts of Section III.

The model distributions E and U are seen to represent the two extreme idealizations of the actual distribution. The rectangular source σ for model E is suggested by the mean hourly echo rates at Jodrell Bank for the continuous survey apparatus (Lovell, loc. cit., p. 115). This equipment has a narrow field of view and the observed echo rates should be dominated by the ecliptical component. This contention is supported by the displacement between the times of occurrence of the diurnal pattern in the two aerials. The ratio in σ of 4 : 1 for the apex and antapex sections of the distribution requires justification. The Jodrell Bank rates suggest a ratio of about 3. A smaller number of counts on the radiant apparatus at Adelaide suggests a ratio of 5, whilst supporting the general shape of the Jodrell Bank variation and also the ecliptical concentration of the meteors detected. The ratios of the maximum to minimum hourly echo rates for the wind equipment (Fig. 6 (*a*)), for a line source (when averaged over all positions of the ecliptic) require a ratio of 4·3. The value of 4 has been chosen as a reasonable compromise between these estimates. Because of aerial smoothing, it was anticipated that little could be gained by attempting to improve upon a rectangular source shape, and a few trials proved this to be the case.

The measure of agreement between actual echo rates and rates predicted for models E and U may be assessed from three aspects : (*a*) general shape of diurnal variation curves ; (*b*) ratio of maximum to minimum hourly echo rate in the diurnal variation ; and (*c*) annual variation of average echo rate per day. Before examining this, it is appropriate to consider the effect of collection in the minor lobe upon these criteria.

For model E, the minor lobe has little effect upon the shape of the diurnal variation near September, but its contribution is very marked near March. This is understandable when it is remembered that at the September equinox at Adelaide the maximum elevation of the apex is 33°, so that collection of meteors from the strong part of the ecliptical source is confined largely to the major lobe. At the March equinox the apex attains an elevation of 79° and the minor lobe is much more important. This dependence of the contribution from the minor lobe on the elevation of the ecliptic is reflected in the annual variations shown in Figure 10 (*a*). It might be thought then that a detailed knowledge of the minor lobe pattern is a prerequisite for predictions based on model E. However, as the ecliptic is in the same position in the sky at 06 hr at the March equinox and 18 hr at the September equinox, and again at 18 hr at March and 06 hr in September, and these times correspond to maxima and

minima in the hourly echo rate, some information regarding the contribution of the minor lobe can be deduced from the observed rates at these times. Thus, if S_{06} denotes the value of $\oint ZdE$ taken along the visible part of the ecliptic (the integral vanishes for the part of the ecliptic below the horizon) at 06 hr in September, then $S_{06}=M_{18}$ and $M_{06}=S_{18}$. Since at these times $\sigma=4$ or 1 for the whole of the visible hemisphere, the ratio of maximum to minimum hourly echo rate during September is $R_S=4S_{06}/S_{18}=4S_{06}/M_{06}$; for March, $R_M=4M_{06}/S_{06}$. Hence

$$R_S/R_M=(S_{06}/M_{06})^2 \quad \ldots\ldots\ldots\ldots\ldots\ldots \quad (8)$$

independent of source strength. But, from what has been said above, the ratio (8) is simply a measure of the contribution of the minor lobe to the echo rate. From Figure 6 (*a*), $R_S/R_M=5\cdot4/3\cdot1=1\cdot7$. For the three functions Z drawn in Figure 8 (*a*), the values of R_S/R_M are :

major lobe only	6·1
major lobe+minor lobe I	1·2
major lobe+minor lobe II	1·8

Because of aerial and source smoothing, the exact shape of the minor lobe pattern is not of major consequence, and discussion of model E may proceed on the basis of the minor lobe II as drawn in Figure 8 (*a*).

For the models U, the presence of the minor lobe fills out and sharpens the maxima in the diurnal variation curves ; the minor lobe is important only whilst the apex lies above the horizon. The ratio of maximum to minimum hourly echo rate (Fig. 12) is much less strongly influenced by the minor lobe than is this ratio for model E ; and the annual variation in average echo rate per day is the same with or without collection in the minor lobe.

The diurnal variations in echo rates predicted for models U are symmetrical about 06 and 18 hr. The asymmetries in the observed diurnal variations definitely favour a non-uniform source, but there is no detailed correspondence between the observations and the curves of Figure 9 for model E. Model E with minor lobe II gives a good account of the annual variation in the ratio of maximum to minimum hourly echo rate, as well as its absolute value. Model U_{42} is more in accord with the observed ratio than U_{35}.

It appears then that the rates and directions of detection of sporadic meteors down to the 7th magnitude are consistent with a distribution which is a combination of models E and U_{42}, i.e. a combination of (*a*) a concentration of radiants to the plane of the ecliptic with further concentration to apex, Sun, and antisun and (*b*) a broader distribution whose apparent degree of concentration to the apex is similar to that of a uniform distribution in space of near-parabolic orbits modified by the Earth's motion. The observed counts in themselves provide no basis for determination of the heliocentric velocities in either of these two components, nor of the ratios of direct to retrograde orbits. However, these two properties of the distributions are not independent in their effects on the distribution.

Thus, if it is postulated, in the light of the radiant distribution of Prentice and the radar survey at Jodrell Bank, that the ecliptical concentration dominates,

the apparent distribution of sporadic radiants is the rectangular line source defined earlier, with apex/antapex density ratio of 4. The true distribution of the radiants round the ecliptic is found by correcting for the Earth's motion, as already described in connexion with models U. For parabolic velocities (42 km/sec) the apparent apex/antapex density ratio 4 implies a true density ratio of 1/9, i.e. the true density of radiants in the direction of the antapex exceeds that in the direction of the apex by a factor of 9. For heliocentric velocity 35 km/sec, the true density ratio is 40, again in favour of the antapex. These ratios imply a very great preponderance of direct orbits. Further, these ratios have been calculated on the assumption that ionizing efficiency is independent of velocity. If instead the ionizing efficiency varies strongly with velocity (say $n=5$), then the above true density ratios will be increased considerably, and could easily be as large as the factors 1000–5000 suggested by Levin (1955) from analysis of visual data. The cause is the same: luminous or ionizing efficiency highly dependent on velocity.

For the sake of argument, let us now consider the more unlikely supposition that the ecliptical component is negligible. If the velocities in the uniform component are much lower than parabolic, the higher degree of concentration to the apex implied by the lower velocities can only be compensated by providing an additional contribution near the antapex, i.e. by increasing the proportion of direct orbits.

Since there is no way of assessing the relative contributions of the two components to the total distribution, these arguments can scarcely be taken any further. If, in the light of the investigations reviewed in Section I, a proportion of short-period orbits with velocities well below the parabolic limit is accepted, then the present work implies a preponderance of direct orbits, whose actual proportion will depend on the details of the velocity distribution and the ionizing efficiency function.

Although the distribution of the orbits cannot be specified in greater detail, firm conclusions may be drawn, from the echo rates alone, regarding the distribution of sporadic meteors round the Earth's orbit. Firstly, attention has already been drawn to the repetition, year after year, of much of the finer detail in the diurnal variation for a given month. This suggests minor fluctuations in the density of sporadic radiants round the Earth's orbit, which persist from year to year. Possibly minor showers, not resolved by the equipment, are involved. However, a detailed study (unpublished) of the day-to-day variations in the activity during the month of October, from 1952 to 1955, suggests some permanent irregularities in the distribution which cannot be due to showers, even minor ones. Secondly, the average echo rate per day, when corrected for equipment sensitivity, changes only slightly for the same month from year to year. Bullough (1954), from an analysis of the Jodrell Bank continuous survey, also agrees that the sporadic activity remains constant from year to year. Thirdly, the annual variations in the average echo rate per day, as predicted by models E and U respectively, are almost identical. If the observed average echo rates of Figure 6 (*b*) are corrected for the variations imposed by the motion of the Earth, the resultant variation should represent the true density of sporadic

meteors round the Earth's orbit. Corrections have been applied for both models E and U_{42} and the resultant density functions are plotted in Figure 13, as departures from the average echo rate per year. Also shown is the density function found from the telescopic surveys based on Skalnaté Pleso (Kresáková and Kresák 1955). The agreement between the two surveys is excellent, and is further strengthened by the agreement between the Skalnaté Pleso survey and Hoffmeister's visual survey (not reproduced).

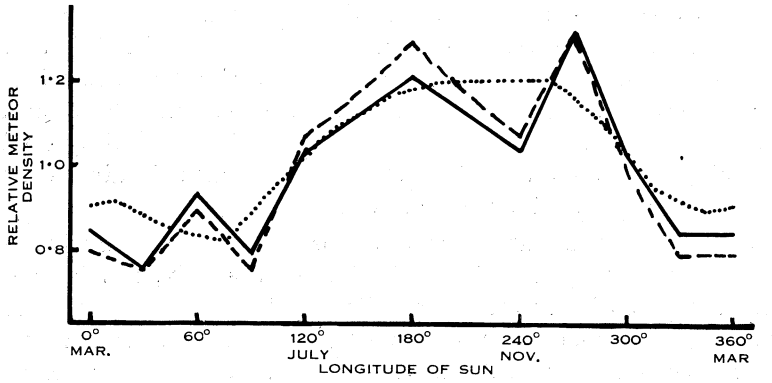

Fig. 13.—Relative density distribution of sporadic meteors round the Earth's orbit. Adelaide model E ——; Adelaide model U_{42} – – –; Skalnaté Pleso telescopic survey · · · ·.

This accordance between surveys using different techniques and made at different times leaves little doubt that the density of sporadic meteors from ⊙120 to ⊙300 is considerably higher than over the remainder of the Earth's orbit. Only the Jodrell Bank radio surveys, which indicate maximum density between ⊙30 and ⊙150, are at variance with this conclusion. It is possible that this disagreement is due to the dominating influence of the sporadic activity associated with the summer day-time showers.

VII. Acknowledgments

This work forms part of the meteor research programme of the University of Adelaide. The project is financed jointly by the University of Adelaide, the Division of Radiophysics, C.S.I.R.O., and the Radio Research Board, C.S.I.R.O. The author wishes to thank Professor L. G. H. Huxley for the generous provision of facilities, and the many members of the research staff of the Department of Physics, University of Adelaide, who have assisted in the operation of the equipment, in data reduction, and in computations.

VIII. References

Almond, M., Davies, J. G., and Lovell, A. C. B. (1953).—*Mon. Not. R. Astr. Soc.* **113**: 110.

Bok, B. J. (1955).—*Sky & Telesc.* **15**: 21.

Browne, I. C., Bullough, K., Evans, S., and Kaiser, T. R. (1956).—*Proc. Phys. Soc. Lond.* B **69**: 83.

Bullough, K. (1954).—*Jodrell Bank Ann.* **1**: 68.

Clegg, J. A. (1948).—*Phil. Mag.* **39**: 577.

DAVIDSON, M. (1914).—*J. Brit. Astr. Ass.* **24**: 352.
ELFORD, W. G., and ROBERTSON, D. S. (1953).—*J. Atmos. Terr. Phys.* **4**: 271.
EVANS, S., and HALL, J. E. (1955).—"Meteors." (Ed. T. R. Kaiser.) p. 18. (Pergamon Press: London.)
KAISER, T. R. (1953).—*Advanc. Phys.* **2**: 495.
KAISER, T. R. (1954).—*Observatory* **74**: 195.
KRESÁK, L. (1955).—*Contributions of the Astronomical Observatory, Skalnaté Pleso.* **1**: 9.
KRESÁKOVÁ, M., and KRESÁK, L. (1955).—*Contributions of the Astronomical Observatory, Skalnaté Pleso.* **1**: 40.
LEVIN, B. J. (1955).—"Meteors." (Ed. T. R. Kaiser.) p. 131. (Pergamon Press: London.)
LOVELL, A. C. B. (1954).—"Meteor Astronomy." (Clarendon Press: Oxford.)
ROBERTSON, D. S., LIDDY, D. T., and ELFORD, W. G. (1953).—*J. Atmos. Terr. Phys.* **4**: 255.
WEISS, A. A. (1955).—*Aust. J. Phys.* **8**: 148.
WHIPPLE, F. L. (1955).—*Astrophys. J.* **121**: 240.

APPENDIX I

The Probability of Detection of Meteor Trails close to the Limiting Line Density α_0

It is implicit in the derivation of expression (**6**) that every meteor which produces a trail whose line density of electrons exceeds the limiting density α_0 is detected by the equipment. The validity of this assumption is now examined. The analogous problem for a pulsed radar equipment, the probability of detection of an echo whose lifetime approaches the pulse separation, has been treated by Bullough (1954).

The recording equipment is triggered by a change in receiver output which exceeds $\frac{1}{3}$ of the constant output due to the ground wave. The change in receiver output produced by a sky wave (echo) of given amplitude depends upon the radio-frequency phase of the sky wave relative to the ground wave. The relative phases of sky and ground waves are slowly shifted by the drift of the meteor trail. It is clear that a sky wave, whose amplitude exceeds $\frac{1}{3}$ that of the ground wave, when combined vectorially with the ground wave may produce a resultant receiver output which changes the normal output by less than $\frac{1}{3}$. If further the trail is close to limiting line density, the sky wave may decay before the drift of the trail carries the phase of the sky wave, and hence the receiver output, to a value such as to trigger the recorder. Under these circumstances echoes will be missed.

If S is the amplitude of the sky wave (G.W.=1) and θ the phase angle between sky and ground waves, then echoes are detected only when

$$\left.\begin{aligned} 1 \geqslant \cos\theta > (7/9 - S^2)/2S, \\ -1 \leqslant \cos\theta < -(5/9 + S^2)/2S. \end{aligned}\right\} \quad \ldots\ldots\ldots\ldots \quad (9)$$

The period T of rotation of θ is determined by the line-of-sight component V_r of the drift velocity of the trail; the relation between them is

$$T = 5 \cdot 6/V_r \quad \ldots\ldots\ldots\ldots\ldots\ldots \quad (10)$$

(Robertson, Liddy, and Elford 1953). Using (**9**) and (**10**), the length of "dead time", when the equipment will not respond to an echo of amplitude S, is

plotted in Figure 14 for several values of V_r. The discontinuity at $S=5/3$ is caused by the replacement of two sections of " dead time " per cycle by only one such section when $S>5/3$.

The amplitude S of an actual echo decays according to the exponential law

$$S=S_0 \exp(-16\pi^2 Dt/\lambda^2),$$

where D is the diffusion coefficient. The time t_d for a decay-type echo of initial amplitude S_0 to decay to $\frac{1}{3}$ is

$$t_d=0\cdot79\times10^4 D^{-1} \ln(3S_0). \quad \ldots\ldots\ldots\ldots \quad (11)$$

This relation is also plotted in Figure 14 for typical values of D.

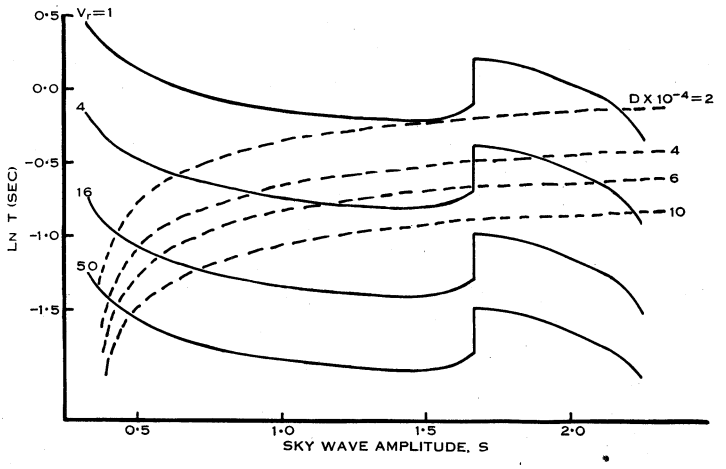

Fig. 14.—Curves for the " dead time " problem. " Dead time " curves for various line-of-sight trail velocities V_r (m/sec) ——; echo decay curves for various diffusion coefficients D – – –. Echoes may be missed if the " dead time " curve appropriate to an echo falls above the decay curve.

An echo may not be recorded if the " dead time " curve lies above the t_d curve. In practice both V_r and D (hence t_d) are highly variable, and it is scarcely worth while assessing accurately the probability of detection of trails, with given V_r and D, close to the limiting line density. On the whole, however, small values of V_r are much more probable at low zenith angles of detection, as the atmospheric wind is closely horizontal, whilst D would be expected to be independent of zenith angle. Hence we reach the conclusion, indicated in the text, that more detectable echoes are missed at low than at higher zenith angles of detection. The inability of the equipment to detect the short, decay-type echoes near the limits of the major lobe will also act in the same sense.